Article

Not peer-reviewed version

Electrochemical Analysis of Corrosion Resistance of Manga-nese-Coated Annealed Steel: Chronoamperometric and Volta-metric Study

Francisco Augusto Nuñez Perez *

Posted Date: 6 August 2024

doi: 10.20944/preprints202408.0368.v1

Keywords: Electrochemical; Corrosion Resistance; Annealed Steel Electrodes

 doi:10.20944/preprints202408.0368.v1

Article

Electrochemical Analysis of Corrosion Resistance of Manganese-Coated Annealed Steel: Chronoamperometric and Voltametric Study

F. A. Núñez-Perez

Universidad Politécnica de Lázaro Cárdenas, Michoacán (Mexico); augusto@uplc.edu.mx

Abstract: Metal corrosion poses a significant challenge for industries by decreasing the lifespan of materials and escalating maintenance and replacement costs. This study is critically important as it assesses the corrosion resistance properties of annealed steel wire electrodes coated with manganese, employing chronoamperometry and linear voltammetry techniques. The electrodes were immersed in an electrolyte solution and subjected to chronoamperometry at various voltages (-0.55 V, -0.60 V, and -0.70 V) and durations (60 seconds and 1800 seconds). Subsequently, linear voltammetry was performed over a potential range from -0.8 V to 0.8 V to generate Tafel plots. The Butler-Volmer equation was applied to the data obtained to determine the corrosion current density. The results indicate that the optimal conditions for forming a highly effective protective manganese layer occur at a potential of -0.70 V for 1800 seconds. Under these conditions, the electrodes exhibited superior corrosion resistance. The study also revealed that shorter durations and less negative potentials led to less effective manganese coatings, with higher corrosion rates and reduced stability. These findings are significant for developing efficient corrosion protection methods in industrial and research applications, providing clear parameters for optimizing the manganese electrodeposition process on annealed steel.

Keywords: electrochemical; corrosion resistance; annealed steel electrodes

1. Introduction

Manganese sulfate monohydrate is a widely used inorganic compound in agriculture as a fully soluble fertilizer [1]. However, beyond its agronomic benefits, manganese holds significant potential in the field of electrochemical corrosion protection [2-3]. Corrosion is the degradation of metals due to chemical or electrochemical reactions with their environment, leading to continuous wear and potential material failure over time [4-7].

This degradation is a critical concern in various industrial applications where the integrity and longevity of metal structures are paramount [8-9]. In coastal environments, the corrosion of structural steel is exacerbated due to high humidity levels, accelerating corrosion and increasing maintenance and repair costs. Recent studies have shown that the cost of corrosion represents a significant percentage of the global GDP, and substantial annual savings could be achieved by implementing available corrosion control techniques [10-11].

Manganese, as a corrosion inhibitor, offers a promising solution. Manganese compounds can form protective films on metal surfaces, acting as barriers that limit the interaction between the metal and the corrosive environment. Additionally, manganese can participate in electrochemical reactions that alter the base metal's corrosion potential, making it less susceptible to oxidation. This ability to modify the electrochemical environment is particularly useful in systems where continuous and effective corrosion protection is required [2-3].

It has been demonstrated that the implementation of manganese compounds can significantly improve the corrosion resistance of metal structures. However, despite the solid foundation provided by previous studies, there is limited information on optimizing electrodeposition conditions and their impact on the long-term durability of manganese coatings [4-9]. A significant part of electrochemistry focuses on optimizing the application of manganese compounds for corrosion protection, evaluating

 doi:10.20944/preprints202408.0368.v1

their effectiveness under different environmental conditions and on various materials. This includes studies on film formation kinetics, film adherence under dynamic conditions, and interactions with other elements present in industrial environments [11-12]. Furthermore, combinations of manganese with other corrosion inhibitors are being explored to create multifunctional protection systems that can offer robust and durable defense against electrochemical degradation.

In summary, integrating manganese into corrosion protection strategies represents a valuable avenue for research and practical application. Ongoing innovation in this field is essential to address the persistent challenges that corrosion poses to industrial infrastructure, ensuring the integrity and longevity of metal structures in various critical applications. Future developments in corrosion protection technologies will not only enhance industrial sustainability and economics but also contribute to long-term safety and environmental protection.

This study explored various methodologies to investigate the electrochemical properties of manganese coatings in protecting annealed steel electrodes against corrosion. The chosen approach focused on oxidation and reduction reactions, using advanced electrochemical techniques to deposit and evaluate manganese coatings [13]. Three types of electrodes were employed in the electrochemical cell setup: a working electrode, a reference electrode, and a counter electrode.

Working Electrode: This is the site of reduction where metal ions are deposited and the desired electrochemical reaction occurs. In this study, annealed steel wire was used as the working electrode. Reference Electrode: It maintains a stable and known potential, serving as a reference point for measuring the working electrode's potential. An Ag/AgCl electrode was used due to its stable potential in aqueous solutions. Counter Electrode: Made of a material with negligible electrochemical activity, the counter electrode completes the electrical circuit and allows current flow through the cell. Graphite was chosen for its inert properties in the studied electrochemical reactions.

The objective of this research was to optimize the conditions for manganese electrodeposition on annealed steel to enhance corrosion resistance. Using chronoamperometry and linear voltammetry techniques, the study systematically investigated the effect of various voltages and durations on the formation and effectiveness of manganese coatings. The results provide a comprehensive understanding of electrochemical corrosion protection, offering practical insights into improving the performance and durability of metallic materials used in industrial and research applications [13].

Moreover, electrodeposition is a low-cost alternative that offers a high degree of control during nucleation and growth, without requiring hazardous experimental conditions [14-16]. Steel is widely used in industry due to its low cost and recyclability, though its low corrosion resistance limits its use. To protect it, galvanized coatings are applied, with electrodeposition being a common technique [17]. Advanced electrochemical techniques, including chronoamperometry and linear voltammetry, were utilized to analyze and characterize the kinetics of corrosion [18-19].

2. Materials and Methods

This work focuses on the corrosion properties of manganese coatings electrodeposited on annealed steel wires using electrochemical methods. The reagents, Manganese Sulfate Monohydrate ($MnSO_4 \cdot H_2O$) and Potassium Chloride (KCl), were purchased from Sigma-Aldrich, ensuring high purity and consistency. Solutions were prepared at concentrations of 0.03 M and 0.09 M, respectively, using deionized water with 18 MΩ·cm resistivity. The manganese electrodeposition was conducted in a three-electrode electrochemical cell. The working electrode was an annealed steel wire, partially covered with silicone or clear enamel, with an exposed section polished with fine sandpaper to ensure a clean, oxide-free surface. The reference electrode was a Metrohm® Ag/AgCl electrode, known for providing a stable and constant reference potential in aqueous solutions [21-22]. The counter electrode was graphite, chosen for its chemical inertness and stability under experimental conditions [23]. All electrodes were meticulously prepared to ensure cleanliness and suitability for electrochemical experiments.

The electrochemical cell temperature was maintained at 25°C using a thermostated water bath, ensuring controlled conditions throughout the experiments. A nitrogen purging system was used to

 doi:10.20944/preprints202408.0368.v1

deoxygenate the solution for 5 minutes before each experiment, preventing unwanted oxidation. The electrochemical experiments were conducted using a rigorously calibrated Metrohm® AUTOLAB PGSTAT302N potentiostat/galvanostat, synchronized with a computer equipped with NOVA software for data acquisition and analysis. This equipment allowed precise control of the applied potentials and the collection of high-quality electrochemical data.

Chronoamperometry experiments were performed at potentials of -0.70 V and -0.60 V for 1800 and 60 seconds, respectively, for manganese deposition. Subsequently, linear voltammetry sweeps from -0.8 V to 0.8 V were carried out in demineralized water to investigate the corrosion rate of the coated electrodes. Cyclic voltammetry curves were obtained through multiple scans to assess the stability and reproducibility of the manganese coating.

The data obtained were analyzed using the Butler-Volmer equation to calculate the corrosion current density (i_{corr}) and corrosion rate. Electrochemical impedance spectroscopy (EIS) was used to generate Nyquist and Bode plots, evaluating charge transfer resistance and double-layer capacitance. These analyses provided a detailed understanding of the efficiency and uniformity of the manganese coatings, allowing optimization of electrodeposition conditions to enhance corrosion resistance.

The reproducibility of the results was verified through the comparison of multiple scans and repeated experiments, ensuring data consistency. Kinetic and thermodynamic parameters, such as Tafel coefficients (b_a and b_c), were determined from logarithmic plots of current density vs. potential. The corrosion current density and corrosion rate were calculated using the Butler-Volmer equation, providing a detailed assessment of corrosion kinetics and manganese coating quality. To calculate the corrosion rate, the following steps and formulas based on electrochemical measurements were used [20-21]: Determination of i_{corr} and E_{corr}

$$i = i_{corr}\left(e^{2.303\frac{E-E_{corr}}{b_a}} - e^{2.303\frac{E-E_{corr}}{k_c}}\right) \qquad (1)$$

where i is the current density, i_{corr} is the current density, E is the applied potential, E_{corr} is the applied potential, b_a is the anodic Tafel slope, b_c is cathodic Tafel slope.

3. Results

3.1. Open Circuit Potential (OCP) Evaluation

The stability and robustness of the Open Circuit Potential (OCP) are fundamental prerequisites for ensuring the consistency and reliability of subsequent electrochemical experiments, such as chronoamperometry and linear voltammetry. The evaluation of the OCP was performed to ensure that the electrodes reached an equilibrium state before the application of external potentials. This equilibrium is crucial for obtaining accurate and reproducible results in the electrochemical analysis[24].

In Figure 1, the Open Circuit Potential (OCP) voltage recorded for manganese-coated annealed steel electrodes is presented. The OCP voltage remained constant over time, indicating high system stability. This stability is critical, as any significant fluctuations in the OCP could adversely affect the outcomes of subsequent experiments.

 doi:10.20944/preprints202408.0368.v1

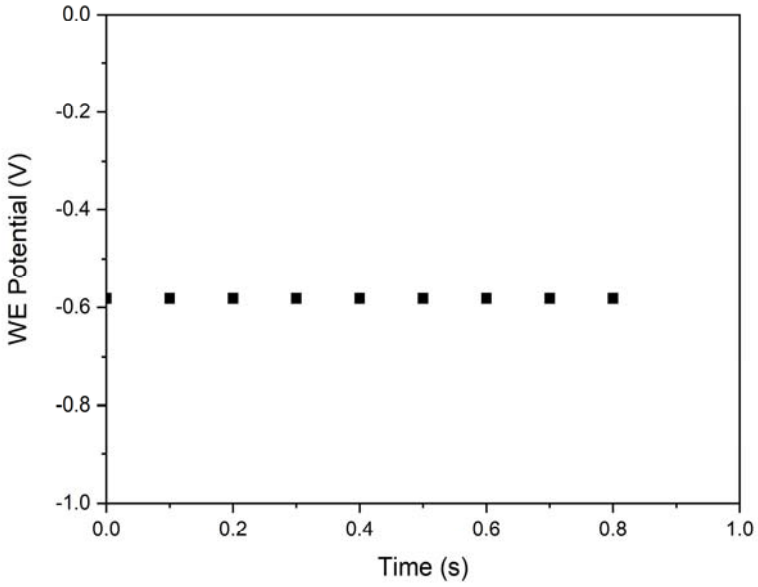

Figure 1. Open Circuit Potential (OCP) Voltage Stability Over Time for Manganese-Coated Steel Electrodes.

The derivative of the working electrode voltage (dWE/dt) is shown in Figure 1(b). A near-zero derivative value indicates a stable OCP, confirming that the system is in equilibrium. This equilibrium condition is essential for initiating chronoamperometry and voltammetry experiments, ensuring consistent and reproducible initial conditions.

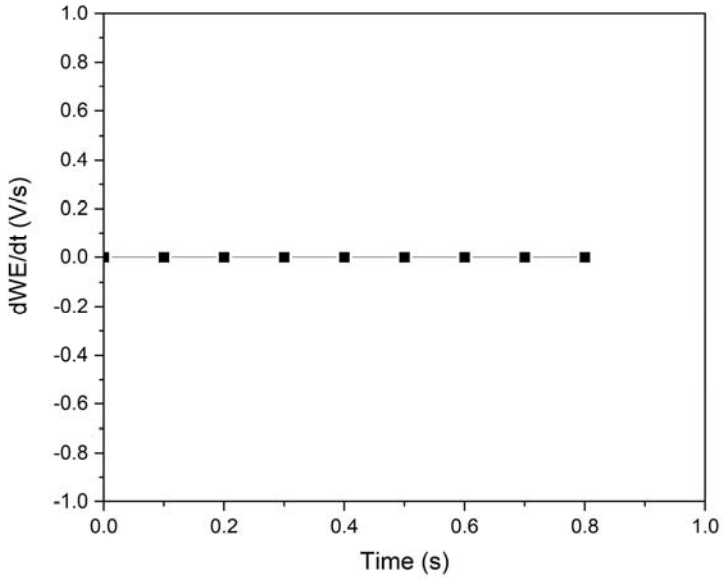

Figure 2. Derivative of the Working Electrode Voltage (dWE/dt) Indicating System Equilibrium.

3.2. Cyclic Voltammetry

The Figure 3 shows the cyclic voltammetry curves obtained over a potential range of -0.8 V to 0.8 V for annealed steel electrodes in manganese sulfate and potassium chloride solutions. The curves from three consecutive scans (Scan 1, Scan 2, Scan 3) exhibit remarkable reproducibility, indicating well-controlled experimental conditions. The current density consistently increases with the applied

 doi:10.20944/preprints202408.0368.v1

potential, characteristic of systems with significant redox processes. The proximity of the observed reduction potential to the OCP suggests that the reduction of Mn^{2+} to Mn occurs near equilibrium conditions, which is ideal for maximizing deposition efficiency. The similarity across the three scans indicates system stability and consistent working electrode surface characteristics, which are crucial for the reproducibility of results.

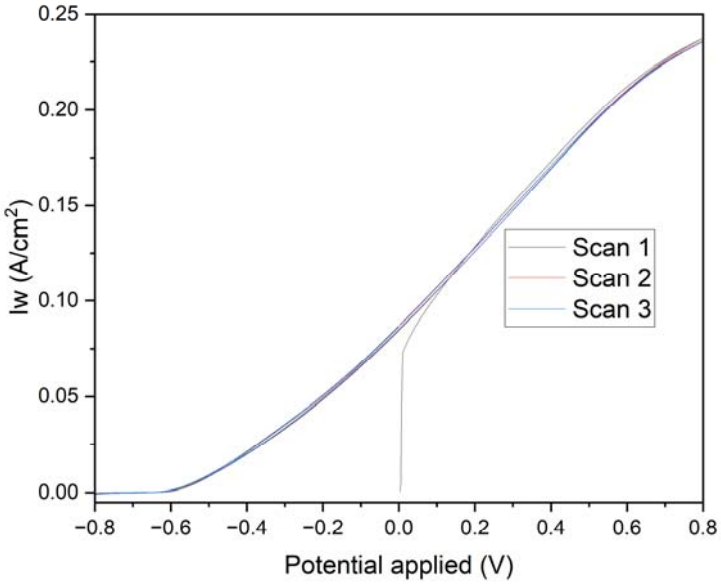

Figure 3. Cyclic Voltammetry Curves for Manganese-Coated Steel Electrodes.

The Figure 4 shows the cyclic voltammetry curves obtained over a potential range of -0.8 V to 0.8 V for annealed steel electrodes in manganese sulfate and potassium chloride solutions. The curves from three consecutive scans (Scan 1, Scan 2, Scan 3) exhibit remarkable reproducibility, indicating well-controlled experimental conditions. The current density consistently increases with the applied potential, characteristic of systems with significant redox processes. The proximity of the observed reduction potential to the OCP suggests that the reduction of Mn^{2+} to Mn occurs near equilibrium conditions, which is ideal for maximizing deposition efficiency. The similarity across the three scans indicates system stability and consistent working electrode surface characteristics, which are crucial for the reproducibility of results.

 doi:10.20944/preprints202408.0368.v1

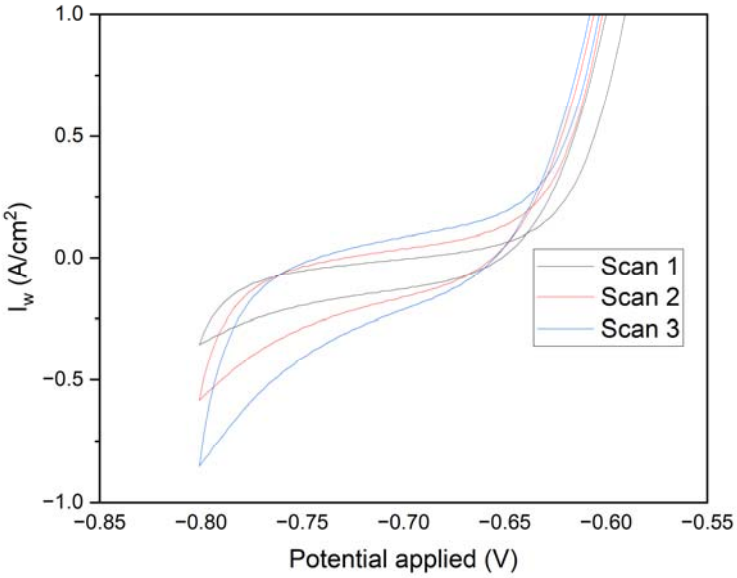

Figure 4. Detail of Potential Range for Mn^{2+} to Mn Reduction Reactions.

Figure 5 presents the cyclic voltammetry curves for annealed steel electrodes, with the natural logarithm (ln) applied to the current density (Iw). Three consecutive scans (Scan 1, Scan 2, and Scan 3) were conducted over a potential range of -0.85 V to -0.55 V to identify kinetically controlled processes and evaluate charge transfer behavior in the reduction and oxidation of Mn^{2+}.

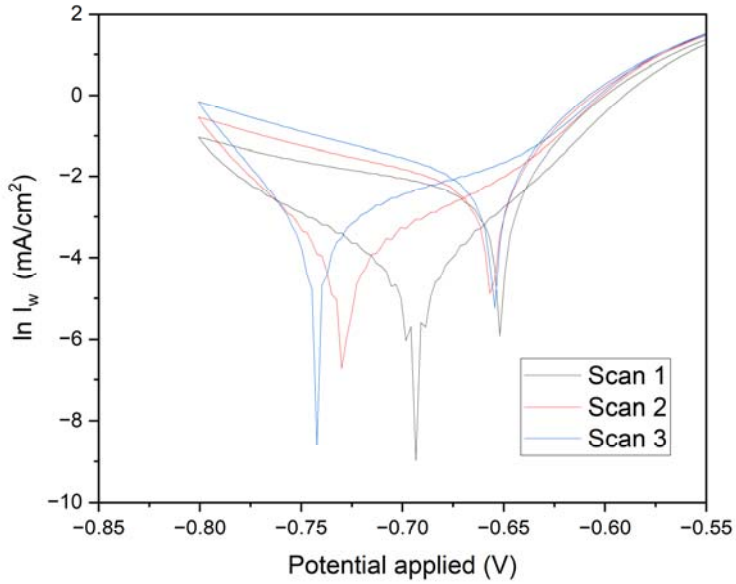

Figure 5. Cyclic Voltammetry Analysis with Logarithmic Transformation.

The logarithmic transformation clarifies changes in current density, enhancing the visualization and analysis of charge transfer processes and kinetically controlled behaviors in the electrochemical system. The curves exhibit a characteristic inverted "V" shape, indicating the presence of reversible redox processes, with a minimum in the cathodic region followed by an ascending section corresponding to anodic oxidation. This behavior is typical in electrochemical systems with alternating reduction and oxidation processes.

 doi:10.20944/preprints202408.0368.v1

The observed minima correspond to cathodic peaks where Mn^{2+} is reduced to metallic Mn. The subsequent ascending sections represent the reoxidation of metallic Mn back to Mn^{2+}.

3.3. Chronoamperometry

The potential of -0.70 V was chosen due to its proximity to the cathodic peak observed in cyclic voltammetry, where the reduction of Mn^{2+} to Mn is most pronounced. This potential ensures effective and consistent Mn^{2+} reduction, providing excellent manganese coverage on the electrode, which is crucial for maximizing corrosion resistance.

The potential of -0.60 V was selected to explore a slightly less negative range, assessing the efficiency of Mn^{2+} reduction under conditions with significant cathodic current but reduced capacitive and transient effects. This allows for a precise comparative evaluation of the manganese coating's quality and characteristics formed under different electrochemical conditions.

The potential of -0.55 V was chosen to investigate the system's behavior at an even less negative potential, where Mn^{2+} reduction is less favorable. This helps to evaluate the impact of a potential closer to the OCP on manganese coating formation, determining the minimum energy required for effective reduction and allowing for critical comparison with results at -0.70 V and -0.60 V.

The Figure 6 shows the current density (Iw) versus time for three applied potentials. At -0.55 V (black line), the initial current density is approximately 150 μA/cm², gradually increasing to over 250 μA/cm² by the experiment's end. This behavior indicates significant oxidation on the annealed steel electrode, likely described by the reaction:

$$Fe\ (s) \rightarrow Fe^{2+}_{(aq)} + 2e^{-} \qquad (2)$$

The KCl in the solution enhances ionic conductivity, facilitating ion transport and improving the kinetics of electrochemical reactions. Cl^- ions can penetrate oxide layers on metals, promoting the formation of soluble corrosion products and continuous iron oxidation.

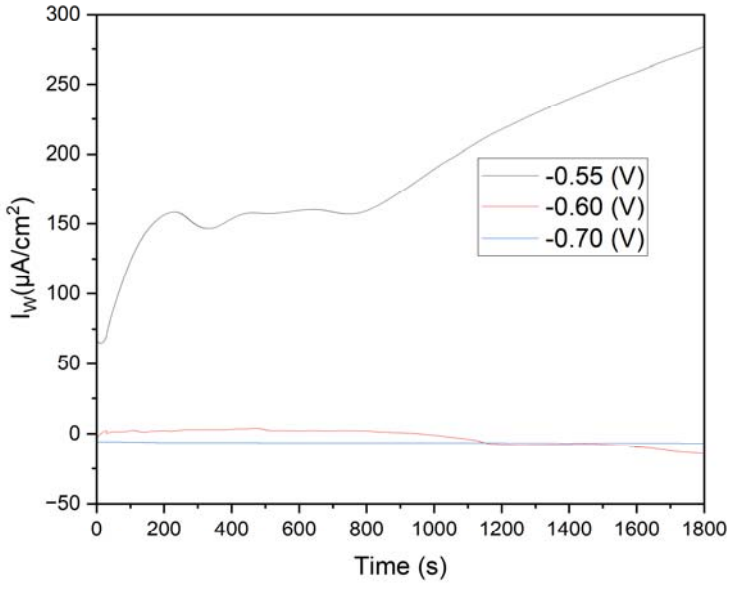

Figure 6. Chronoamperometry at -0.55 V, -0.60 V, and -0.70 V.

Effect of Manganese Sulfate ($MnSO_4 \cdot H_2O$): Mn^{2+} in the solution can influence passive layer formation on steel. While Mn^{2+} ions do not directly participate in iron oxidation, their presence can alter the properties of the oxide film, potentially making it more porous and allowing sustained oxidation.

 doi:10.20944/preprints202408.0368.v1

The Figure 7 displays the chronoamperometry curves obtained at potentials of -0.60 V and -0.70 V over 1800 seconds. The variations in current density highlight critical differences in electrochemical behavior and the effectiveness of Mn^{2+} reduction under different potential conditions.

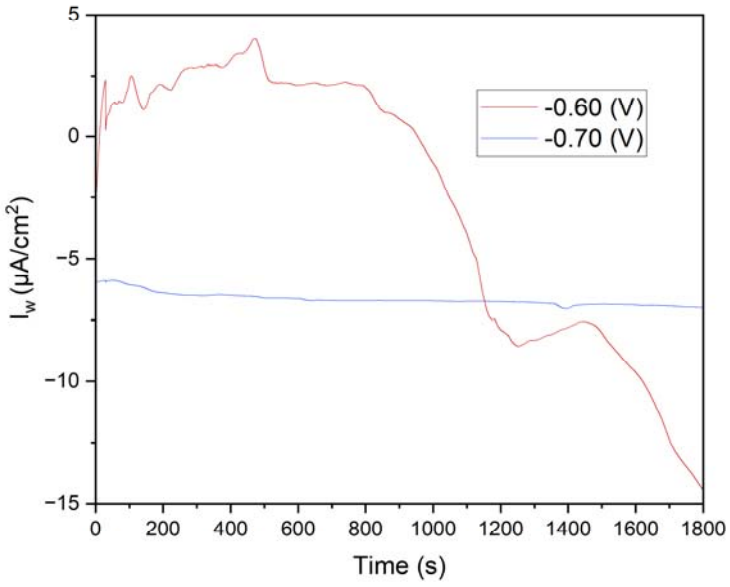

Figure 7. Chronoamperometry at -0.55 V, -0.60 V, and -0.70 V.

This study confirms that chronoamperometry at varying potentials accurately evaluates manganese electrodeposition efficiency and its impact on the corrosion resistance of annealed steel. Results show that -0.70 V provides uniform and highly effective manganese coverage, significantly reducing corrosion current density. $MnSO_4 \cdot H_2O$ and KCl solutions play crucial roles in coating formation and stability, enhancing the protective properties of the steel electrode.

These findings provide a robust basis for optimizing manganese electrodeposition conditions, improving the durability and corrosion resistance of metallic coatings in industrial and research applications. A detailed understanding and control of these electrochemical processes are essential for advancing corrosion protection, significantly extending the lifespan of critical metal structures.

3.4. Linear Voltammetry

The Figure 8 presents linear voltammetry curves for electrodes subjected to different chronoamperometric treatments, providing critical insights into the electrochemical behavior and surface characteristics of the deposited manganese layers. The initial negative currents observed in the curves are attributed to the reduction of oxidized species present on the surface of the deposited manganese or impurities in the medium. The likelihood of water reduction at these potentials with the electrodes used is negligible. As the potential becomes less negative and transitions to positive, the reversal of the current clearly indicates the oxidation of the deposited manganese or the underlying iron. The specific reactions involved are:

$$\text{Oxidation of Manganese: } Mn \rightarrow Mn^{2+} + 2e^- \quad (3)$$

$$\text{Oxidation of Iron: } Fe\ (s) \rightarrow Fe^{2+} + 2e^- \quad (4)$$

Electrodes polarized at -0.70 V for 1800 seconds (Black Line): These electrodes exhibit a controlled and gradual transition, reflecting a more stable protective manganese layer. The steady increase in current towards positive values, without significant parasitic reactions, confirms the excellent corrosion resistance provided by the uniform and well-adhered manganese coating.

 doi:10.20944/preprints202408.0368.v1

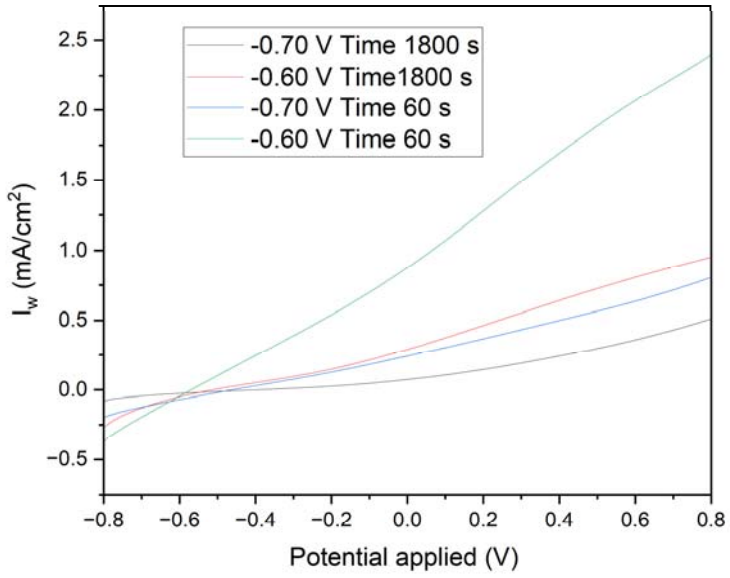

Figure 8. Linear Voltammetry Curves Under Different Chronoamperometric Conditions.

Electrodes polarized at -0.60 V for 1800 seconds (Red Line): A similar pattern is observed with these electrodes, albeit with a smaller initial negative current, indicating a less oxidized initial layer. This results in slightly reduced corrosion resistance compared to the electrodes treated at -0.70 V. The manganese layer formed under these conditions, while still protective, shows marginally less effectiveness in corrosion prevention.

Electrodes polarized at -0.70 V for 60 seconds (Blue Line): The pronounced initial negative current, followed by a rapid increase to positive values, highlights a quick reduction of surface species and subsequent oxidation. This behavior indicates a less uniform deposition process, resulting in a thinner and less consistent manganese layer, which compromises the corrosion protection.

Electrodes polarized at -0.60 V for 60 seconds (Green Line): These electrodes demonstrate a rapid rise in current density from slightly negative to positive values. This indicates minimal initial reduction and a swift oxidation process, revealing significant transient and capacitive effects. The manganese layer produced is discontinuous and less protective, offering inadequate corrosion resistance.

The initial negative currents are unequivocally linked to the reduction of oxidized surface species or impurities, while water reduction is not a significant factor at these potentials. As the potential becomes less negative and turns positive, the observed current inversion signifies the oxidation of the deposited manganese or iron substrate. The clearly defined electrochemical reactions highlight the critical role of chronoamperometric parameters in determining the integrity and protective quality of the deposited manganese layer. Electrodes subjected to -0.70 V for longer durations (1800 seconds) form a more stable and protective manganese layer, whereas shorter times and less negative voltages lead to inferior layers with rapid oxidation transitions, indicating a lower protective quality.

This analysis underscores the necessity of optimizing chronoamperometric conditions to enhance the corrosion resistance of manganese coatings, essential for practical applications.

The Figure 9 presents crucial data on current density versus time, elucidating the quality of manganese electrodeposition and its impact on the corrosion resistance of annealed steel electrodes. The results clearly demonstrate that optimal conditions for effective electrodeposition and enhanced corrosion resistance are achieved with a duration of 1800 seconds at -0.70 V. In this study, the corrosion properties of annealed steel wire electrodes, subjected to various chronoamperometric

 doi:10.20944/preprints202408.0368.v1

conditions, were thoroughly evaluated. Following the treatment, the electrodes were immersed in demineralized water, and linear voltammetry tests were conducted from -0.8 V to 0.8 V. The resulting graph, depicted on a logarithmic scale of current density, allows for the analysis of Tafel characteristics and corrosion kinetics.

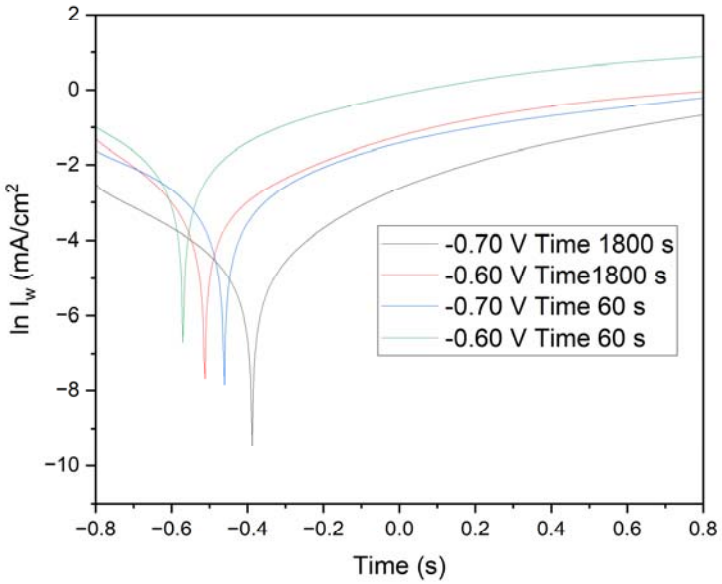

Figure 9. Tafel Plots Obtained via Linear Voltammetry (Ln(Current Density) vs. Potential) for Annealed Steel Electrodes under Different Chronoamperometric Conditions.

Electrodes subjected to -0.70 V for 1800 seconds (black line): These electrodes exhibit a deep minimum followed by a gradual recovery. The linear section of the curve in the cathodic region provides detailed insights into the corrosion rate and kinetic parameters of reduction.

Electrodes subjected to -0.60 V for 1800 seconds (red line): Similar behavior is observed, with a less pronounced minimum and a smaller slope in the cathodic region, indicating lower reductive activity.

Electrodes subjected to -0.70 V for 60 seconds (blue line): These display a significant minimum followed by a rapid recovery, suggesting a fast initial reduction and less controlled subsequent oxidation.

Electrodes subjected to -0.60 V for 60 seconds (green line): The current density rapidly increases from a minimum to positive values, indicating lower corrosion resistance and less effective reduction kinetics.

Cathodic and Anodic Peaks: The minima in the curves represent cathodic peaks where the reduction of oxidized species on the deposited manganese occurs. The subsequent recovery indicates the onset of oxidation processes. The position and depth of these peaks are critical indicators of the efficiency of the reduction process and the quality of the protective manganese coating.

Linear Regions and Tafel Slopes: The linear sections on the logarithmic scale provide the Tafel slopes, essential for determining kinetic parameters such as the charge transfer coefficient (β) and the exchange current density (i_0). These parameters indicate the ease with which the redox reaction occurs. Electrodes subjected to -0.70 V for 1800 seconds exhibit steeper Tafel slopes and deeper minima, suggesting higher efficiency in reduction and superior manganese coating quality. Conversely, electrodes subjected to -0.60 V for 60 seconds show shallower slopes and quicker recovery, indicating lower reduction efficiency and increased corrosion susceptibility.

Scan Comparisons: Comparative analysis reveals that electrodes subjected to -0.70 V for 1800 seconds exhibit the highest corrosion resistance, with more favorable reduction kinetics and a more uniform manganese coating. In contrast, electrodes subjected to -0.60 V for 60 seconds demonstrate

 doi:10.20944/preprints202408.0368.v1

the lowest corrosion resistance, reflecting less effective reduction kinetics and a less uniform protective layer.

The application of the Butler-Volmer equation to the linear voltammetry data has enabled a detailed assessment of corrosion kinetics and manganese coating quality. Optimal conditions for effective electrodeposition and enhanced corrosion resistance are clearly achieved with 1800 seconds at -0.70 V, as demonstrated in Table 1. These electrodes exhibit the lowest corrosion current density and corrosion rate, indicating a highly effective protective manganese layer. These findings are critical for developing efficient corrosion protection methods in industrial and research applications, providing clear parameters for optimizing the manganese electrodeposition process.

Table 1. Corrosion Rate Calculations for Manganese-Electrodeposited Samples.

Chronoamperometric Time (s)	Chronoamperometric Voltage (V)	E_{corr}, obs (V)	J_{Corr} (A/cm^2)	I_{corr} (A)	Corrosion Rate (mm/year)
60	-0.6	-0.56969	0.00044107	8.86E-06	5.1253
1800	-0.6	-0.51283	5.61E-05	5.61E-05	0.65205
60	-0.7	-0.46147	9.94E-05	2.00E-06	1.1549
1800	-0.7	-0.3881	1.21E-05	2.43E-07	0.14023

3.5. Electrochemical Impedance Spectroscopy (EIS) Results

In addition to the Tafel curve analysis, an electrochemical impedance spectroscopy (EIS) study was conducted to evaluate the charge transfer resistance of annealed steel wire in a manganese sulfate monohydrate and KCl solution at the applied voltages during manganese electrodeposition.

This study assessed the electrochemical properties of annealed steel wire in a solution of manganese sulfate monohydrate and KCl using EIS. The specific potentials analyzed were -0.55 V, -0.6 V, and -0.7 V, selected based on prior studies of manganese electrodeposition. The resulting Nyquist plot represents the impedance of the electrodes at the three applied potentials. In this plot, the Z' (Ω) axis corresponds to the real part of the impedance, while the −Z'' (Ω) axis represents the imaginary part (see Figure 10).

Semicircular Shape: The curves exhibit semicircular arcs, characteristic of systems dominated by charge transfer processes. The semicircular shape indicates that charge transfer resistance (R_{ct}) is the predominant process.

 doi:10.20944/preprints202408.0368.v1

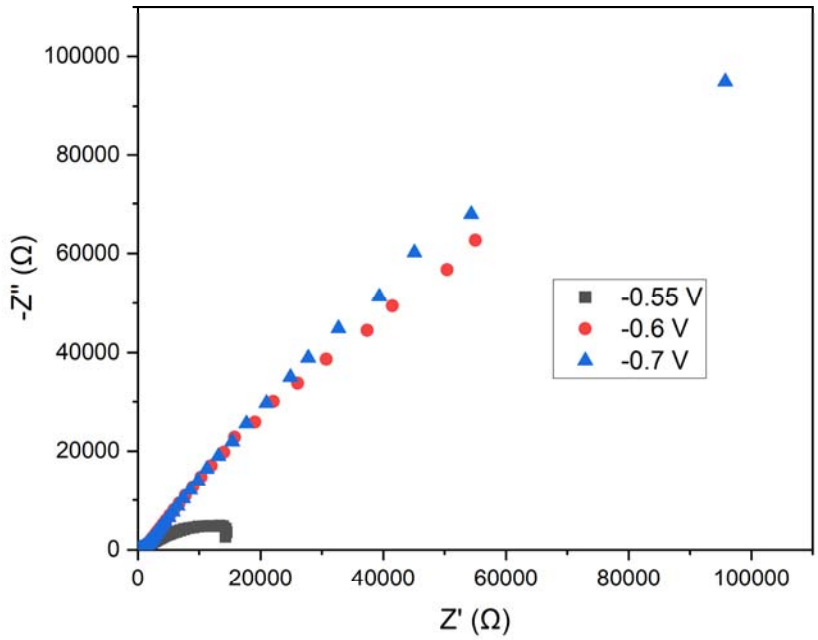

Figure 10. Nyquist Plot for Different Potentials.

Potential Comparison: At -0.55 V (black squares), the impedance is lower compared to -0.6 V (red circles) and -0.7 V (blue triangles), particularly in the high and mid-frequency regions. The impedance at -0.7 V is greater than at -0.6 V, indicating a higher charge transfer resistance.

Charge Transfer Resistance: The lower impedance observed at -0.55 V suggests a reduced charge transfer resistance compared to the other potentials. This could imply a less efficient and uniform manganese electrodeposition at this potential.

Double Layer Capacitance: Variations in impedance may be influenced by changes in the electrochemical double layer capacitance at different potentials. At more negative potentials, the structure of the double layer may be altered, affecting ion distribution and, consequently, the impedance.

Practical Implications: Electrodeposition at -0.7 V, which exhibits the highest charge transfer resistance, suggests more favorable conditions for forming a protective manganese layer. The efficiency of electrodeposition must be balanced with coating stability and deposition rate, which may require further analysis using additional electrochemical techniques such as cyclic voltammetry.

The analysis of the Nyquist plot indicates that a potential of -0.70 V results in the highest charge transfer resistance, potentially correlating with more efficient and uniform manganese electrodeposition on annealed steel wire. In contrast, the potential of -0.55 V exhibits lower charge transfer resistance, which may lead to less effective electrodeposition.

The Figure 11 shows the Bode plot depicting impedance as a function of frequency for the three applied potentials. In this plot, the Z (Ω) axis represents the magnitude of the impedance, while the x-axis represents frequency (Hz) on a logarithmic scale.

 doi:10.20944/preprints202408.0368.v1

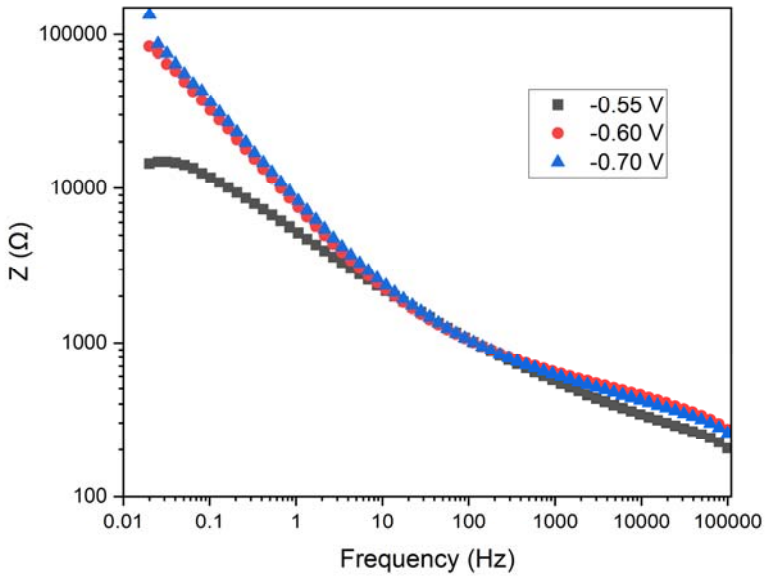

Figure 11. Bode Plot for Different Potentials.

Impedance Behavior: At low frequencies, the impedance is higher, which is typical in electrochemical systems due to the dominance of charge transfer resistance and double layer capacitance. At high frequencies, the impedance decreases, indicating the predominance of electrolyte resistance and inductance of the wiring.

Potential Comparison: At -0.55 V (black squares), the impedance is the lowest at low and mid frequencies compared to the other potentials. At -0.7 V (blue triangles), the impedance is the highest across the entire frequency range, indicating a higher charge transfer resistance. At -0.6 V (red circles), the impedance lies between the other two potentials.

Charge Transfer Resistance: The lowest impedance observed at -0.55 V suggests a lower charge transfer resistance compared to the other potentials, indicating a potentially higher efficiency in electrodeposition at this potential. The higher impedance at -0.7 V indicates a greater charge transfer resistance, suggesting that electrodeposition is less efficient but potentially more uniform and dense.

Double Layer Capacitance: The difference in impedance at various frequencies also reflects the double layer capacitance. Higher impedance at low frequencies indicates a higher double layer capacitance.

Practical Implications: At -0.55 V, the lower charge transfer resistance may result in a faster electrodeposition rate, though the uniformity of the coating could be inferior. At -0.7 V, the higher charge transfer resistance suggests a more controlled and uniform electrodeposition, potentially leading to better coating quality.

The analysis of the Bode plot indicates that a potential of -0.55 V results in the lowest charge transfer resistance, which may lead to faster but less uniform electrodeposition. The potential of -0.7 V shows the highest charge transfer resistance, suggesting more favorable conditions for uniform and controlled manganese electrodeposition. These results are consistent with those observed in the Nyquist plot, reinforcing the hypothesis that a potential of -0.7 V provides the optimal conditions for manganese electrodeposition in terms of coating uniformity and quality.

The Figure 12 illustrates the phase angle of the impedance as a function of frequency at the three applied potentials. In this plot, the vertical axis represents the phase angle (degrees), while the horizontal axis denotes frequency (Hz) on a logarithmic scale.

 doi:10.20944/preprints202408.0368.v1

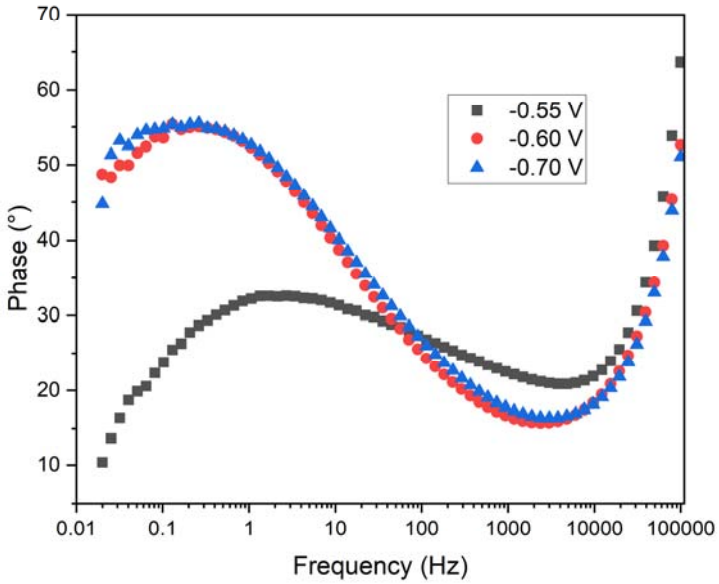

Figure 12. Phase Angle Plot for Different Potentials.

Phase Behavior: The three curves exhibit a bell-shaped characteristic, typical of systems dominated by charge transfer and diffusive processes. At low and high frequencies, the phase angle decreases, indicating resistive behavior. In the mid-frequency range, the phase angle increases, reflecting the capacitive contribution of the double layer.

Potential Comparison: At -0.55 V (black squares), the phase angle reaches its maximum at lower frequencies compared to -0.6 V (red circles) and -0.7 V (blue triangles). The phase maximum at -0.7 V is slightly higher than at -0.6 V, suggesting a greater capacitive contribution.

Charge Transfer Resistance: The position of the phase maximum correlates with the characteristic frequency of the system, influenced by the charge transfer resistance and double layer capacitance. The lower frequency at which the phase maximum occurs at -0.55 V suggests a lower charge transfer resistance compared to the other potentials.

Double Layer Capacitance: The higher phase angle observed at -0.7 V indicates a greater double layer capacitance, potentially related to increased manganese coating coverage. The shape and position of the phase curves indicate differences in the structure and uniformity of the coating formed at different potentials.

Practical Implications: At -0.55 V, the lower charge transfer resistance may facilitate faster electrodeposition, though the coating quality may be inferior. Conversely, at -0.7 V, the higher charge transfer resistance and greater double layer capacitance suggest a more controlled and uniform electrodeposition, potentially resulting in superior coating quality.

The phase angle analysis in Figure 12 reveals that a potential of -0.55 V results in a lower charge transfer resistance, potentially leading to faster, albeit less uniform, manganese electrodeposition. The higher phase angle and greater double layer capacitance at -0.7 V imply a more capacitive interface, consistent with a more uniform and dense manganese deposition. This suggests that electrodeposition at -0.7 V not only improves the uniformity and adherence of the manganese layer but also enhances the protective qualities of the coating by facilitating a more stable and capacitive double layer.

These findings align with the Nyquist and Bode plots, further supporting the conclusion that a potential of -0.7 V offers the optimal conditions for manganese electrodeposition. This potential provides a balanced environment that ensures efficient charge transfer while maintaining a high double layer capacitance, crucial for achieving a consistent and protective manganese layer.

 doi:10.20944/preprints202408.0368.v1

4. Conclusions

This study offers a comprehensive assessment of the corrosion resistance characteristics of annealed steel wire electrodes coated with manganese, utilizing advanced chronoamperometric and linear voltammetric techniques. The results indicate that manganese electrodeposition at a potential of -0.70 V for 1800 seconds produces a highly efficient and uniform protective layer, achieving optimal corrosion resistance. This specific potential and duration facilitate the effective reduction of Mn^{2+} to Mn, resulting in a dense and stable coating that significantly reduces corrosion current density and corrosion rate.

The electrochemical impedance spectroscopy (EIS) analysis corroborates these findings, revealing that electrodes subjected to -0.70 V exhibit the highest charge transfer resistance, indicative of a more controlled and efficient electrodeposition process. In contrast, less negative potentials and shorter chronoamperometric durations resulted in less effective manganese coatings, characterized by increased susceptibility to corrosion and diminished overall stability.

Furthermore, the study underscores the critical role of manganese sulfate monohydrate and potassium chloride in the electrolyte solution. Manganese ions are pivotal in forming a dense and uniform protective layer, while chloride ions enhance ionic conductivity and system stability.

These insights are instrumental for the development of advanced corrosion protection strategies in industrial and research applications. The study provides well-defined parameters for optimizing the manganese electrodeposition process on annealed steel, thereby enhancing the durability and performance of metallic coatings.

Author Contributions: The sole author, F.A. Núñez-Perez, was responsible for all phases of the work reported.

Funding: Please add: This research received no external funding

Data Availability Statement: The original contributions detailed in the study are included in the article; for further information, inquiries can be directed to the corresponding author.

Acknowledgments: I sincerely appreciate the Universidad Politecnica de Lazaro Cardenas for offering me the opportunity and the essential resources to carry out this project.

Conflicts of Interest: The author declare no conflicts of interest

References

1. Walter, K. H. (1988) Manganese fertilizers. In Manganese in Soils and Plants: Proceedings of the International Symposium on 'Manganese in Soils and Plants' Held at the Waite Agricultural Research Institute, The University of Adelaide, Glen Osmond, South Australia, August 22–26, 1988 as an Australian Bicentennial Event (pp. 225-241). Dordrecht: Springer Netherlands.
2. Zhang, Y., Liu, Z., Wang, Y., Zhai, Y., Cui, C., Zhang, Q., ... & Wang, X. (2024). Study on the role of chromium addition on sliding wear and corrosion resistance of high-manganese steel coating fabricated by wire arc additive manufacturing. Wear, 540, 205242. https://doi.org/10.1016/j.wear.2024.205242
3. Machado, P. C., Pereira, J. I., & Sinatora, A. (2021). Abrasion wear of austenitic manganese steels via jaw crusher test. *Wear*, *476*, 203726. https://doi.org/10.1016/j.wear.2021.203726
4. Saji, V. S. (2023). Corrosion and materials degradation in electrochemical energy storage and conversion devices. *ChemElectroChem*, *10*(11), e202300136. https://doi.org/10.1002/celc.202300136
5. Jiang, C., Wu, Y. F., & Dai, M. J. (2018). Degradation of steel-to-concrete bond due to corrosion. *Construction and Building Materials*, *158*, 1073-1080. https://doi.org/10.1016/j.conbuildmat.2017.09.142
6. Wasim, M., Li, C. Q., Mahmoodian, M., & Robert, D. (2019). Mechanical and microstructural evaluation of corrosion and hydro6gen-induced degradation of steel. *Journal of Materials in Civil Engineering*, *31*(1), 04018349. https://doi.org/10.1061/(ASCE)MT.1943-5533.0002560
7. Perez, N., & Perez, N. (2016). Electrochemical corrosion. *Electrochemistry and corrosion science*, 1-23.
8. Bender, R., Féron, D., Mills, D., Ritter, S., Bäßler, R., Bettge, D., ... & Zheludkevich, M. (2022). Corrosion challenges towards a sustainable society. *Materials and corrosion*, *73*(11), 1730-1751. https://doi.org/10.1002/maco.202213140
9. Di Sarno, L., Majidian, A., & Karagiannakis, G. (2021). The effect of atmospheric corrosion on steel structures: A state-of-the-art and case-study. *Buildings*, *11*(12), 571. https://doi.org/10.3390/buildings11120571

10. Loukili, H., Azzaoui, K., Bouyanzer, A., Kertit, S., & Hammouti, B. (2022). Corrosion Inhibition using Green Inhibitors: An Overview. *Maghrebian Journal of Pure and Applied Science*, *8*(2), 82-93. https://doi.org/10.48383/IMIST.PRSM/mjpas-v8i1.29392
11. Koch, G. (2017). Cost of corrosion. *Trends in oil and gas corrosion research and technologies*, 3-30. https://doi.org/10.1016/B978-0-08-101105-8.00001-2
12. [Zhang, T., et al. Synthesis and Electrochemical Properties of Manganese Dioxide as Cathode Material for Aqueous Zinc-Ion Batteries. Russian Journal of Applied Chemistry, 2019, 21, 154-161. https://doi.org/10.1134/S1070427221080115
13. [Lu, J., Dreisinger, D., & Glück, T. (2014). Manganese electrodeposition—A literature review. *Hydrometallurgy*, *141*, 105-116. https://doi.org/10.1016/j.hydromet.2013.11.002
14. Kushwaha, A., & Aslam, M. (2014). ZnS shielded ZnO nanowire photoanodes for efficient water splitting. *Electrochimica Acta*, *130*, 222-231. https://doi.org/10.1016/j.electacta.2014.03.008
15. Skompska, M., & Zarębska, K. (2014). Electrodeposition of ZnO nanorod arrays on transparent conducting substrates–a review. *Electrochimica Acta*, *127*, 467-488. https://doi.org/10.1016/j.electacta.2014.02.049
16. Ruiz-Ocampo, F. D., Zapien-Rodríguez, J. M., Burgara-Montero, O., Escoto-Sotelo, E. A., Núñez-Pérez, F. A., & Ballesteros-Pacheco, J. C. (2017). Electrodeposition of Nanostructured ZnO Photoanodes for Their Application in the Oxygen Evolution Reaction. International Journal of Electrochemical Science, 12(6), 4898-4914. https://doi.org/10.20964/2017.06.74
17. Cabral-Miramontes, J. A., Bastidas, D. M., Baltazar, M. A., Zambrano-Robledo, P., Bastidas, J. M., Almeraya-Calderón, F. M., & Gaona-Tiburcio, C. (2019). Corrosion behavior of Zn-TiO2 and Zn-ZnO electrodeposited coatings in 3.5% NaCl solution. *International Journal of Electrochemical Science*, *14*(5), 4226-4239. https://doi.org/10.20964/2019.05.10
18. Falcón, J. M., & Aoki, I. V. (2024). Electrodeposition of ZnCo alloy coatings on carbon steel and their corrosion resistance. *Surface and Coatings Technology*, *481*, 130603. https://doi.org/10.1016/j.surfcoat.2024.130603
19. Núñez-Perez, F. A. (2024). Electrochemical analysis of the corrosion resistance of annealed steel with nickel coating in marine environment simulations: chronoamperometric and voltametric study. *Ibero-American Journal of Engineering & Technology Studies*, *4*(1), 62-70. https://doi.org/10.56183/iberotecs.v4i1.641
20. Mukherjee, J., Adalder, A., Mukherjee, N., & Ghorai, U. K. (2023). Solvothermal synthesis of α–CuPc nanostructures for electrochemical nitrogen fixation under ambient conditions. Catalysis Today, 423, 113905.https://doi.org/10.1016/j.cattod.2022.09.011
21. Dawkins, R. C., Wen, D., Hart, J. N., & Vepsäläinen, M. (2021). A screen-printed Ag/AgCl reference electrode with long-term stability for electroanalytical applications. *Electrochimica Acta*, *393*, 139043. https://doi.org/10.1016/j.electacta.2021.139043
22. Nigde, M., Agir, I., Yıldırım, R., & Isildak, I. (2022). Development and comparison of various rod-shaped mini-reference electrode compositions based on Ag/AgCl for potentiometric applications. *Analyst*, *147*(3), 516-526. https://doi.org/10.1039/D1AN01754C
23. Cui, Z., & Sheng, W. (2023). Thoughts about choosing a proper counter electrode. *ACS Catalysis*, *13*(4), 2534-2541. https://doi.org/10.1021/acscatal.2c05145
24. Yang, J., Papaderakis, A. A., Roh, J. S., Keerthi, A., Adams, R. W., Bissett, M. A., ... & Dryfe, R. A. (2024). Measuring the Capacitance of Carbon in Ionic Liquids: From Graphite to Graphene. *The Journal of Physical Chemistry C*, *128*(9), 3674-3684. 024 The Authors. Published by American Chemical Society https://doi.org/10.1021/acs.jpcc.3c08269open_in_new